THE JOURNAL OF BIOLOGICAL CHEMISTRY VOL. 281, NO. 48, pp. 36952–36959, December 1, 2006

The Smc5-Smc6 DNA Repair Complex

*BRIDGING OF THE Smc5-Smc6 HEADS BY THE KLEISIN, Nse4, AND NON-KLEISIN SUBUNITS**

Received for publication, August 21, 2006, and in revised form, September 22, 2006 Published, JBC Papers in Press, September 27, 2006, DOI 10.1074/jbc.M608004200

Jan Palecek[1], **Susanne Vidot, Min Feng, Aidan J. Doherty, and Alan R. Lehmann**[2]

From the Genome Damage and Stability Centre, University of Sussex, Falmer, Brighton BN1 9RQ, United Kingdom

Structural maintenance of chromosomes (SMC) proteins play fundamental roles in many aspects of chromosome organization and dynamics. The SMC complexes form unique structures with long coiled-coil arms folded at a hinge domain, so that the globular N- and C-terminal domains are brought together to form a "head." Within the Smc5-Smc6 complex, we previously identified two subcomplexes containing Smc6-Smc5-Nse2 and Nse1-Nse3-Nse4. A third subcomplex containing Nse5 and -6 has also been identified recently. We present evidence that Nse4 is the kleisin component of the complex, which bridges the heads of Smc5 and -6. The C-terminal part of Nse4 interacts with the head domain of Smc5, and structural predictions for Nse4 proteins suggest similar motifs that are shared within the kleisin family. Specific mutations within a predicted winged helix motif of Nse4 destroy the interaction with Smc5. We propose that Nse4 and its orthologs form the δ-kleisin subfamily. We further show that Nse3, as well as Nse5 and Nse6, also bridge the heads of Smc5 and -6. The Nse1-Nse3-Nse4 and Nse5-Nse6 subcomplexes bind to the Smc5-Smc6 heads domain at different sites.

The structural maintenance of chromosomes (SMC)[3] proteins play important roles in sister chromosome cohesion, chromosome condensation, and DNA repair. Three separate SMC protein complexes are conserved in all eukaryotes. Each contains a heterodimeric core of two SMC proteins, together with 2–6 non-SMC proteins. SMC proteins all have a similar structure of globular head domains at the N and C termini joined by long coiled-coil domains to a hinge. The protein folds back on itself at the hinge, such that the two coiled-coil domains intertwine and the N- and C-terminal heads are brought together (Fig. 1*A*). The N- and C-terminal head domains contain Walker A and B motifs, respectively, and bringing the two head domains together generates an ATPase active site. In the heterodimers (and prokaryotic homodimers), the two SMC proteins interact strongly through their hinge regions (1–3). In the case of the cohesin (Smc1-Smc3) complex, the SMC core is thought to form a ring, with the head domains of each monomer bridged with the non-SMC components Scc1 and Scc3 (nomenclature from *Saccharomyces cerevisiae*) (4). The N terminus of Scc1 interacts with Smc3, whereas its C terminus interacts with Smc1. The ring is thought to hold sister chromatids together after DNA replication. Consistent with this idea, Scc1 is cleaved at the metaphase-anaphase transition by a specific protease designated separase (5). This releases the sister chromatids and enables them to separate at anaphase. In a bioinformatic study, Schleiffer *et al.* (6) identified a protein superfamily that they designated "kleisins," whose function, as described above for Scc1, is to bridge the head domains of the two Smc proteins (Fig. 1*A*). Kleisins include the *Bacillus subtilis* non-Smc protein ScpA as well as Scc1 and its orthologs, the latter being termed the α-kleisin subfamily.

A second SMC complex is condensin, which plays an essential role in condensing chromosomes at prophase (1–3). Smc2 and -4 form the core of condensin, and there are three associated non-Smc proteins. Although evidence suggests that condensin may not form a ring structure (7), one of its non-SMC proteins, Brn1, and its orthologs were assigned by bioinformatic analysis to a subfamily of γ-kleisins (6).

The Smc5-Smc6 complex was first identified by the sensitivity of *smc6* (previously designated *rad18*) mutants of *Schizosaccharomyces pombe* to DNA damage, and studies in several laboratories have suggested a role in repair of DNA by homologous recombination (reviewed in Ref. 8). The Smc5-Smc6 complex has been purified from *S. pombe* (9, 10), and four essential non-SMC components, designated Nse1–Nse4, have been identified (10–16) as well as two further components (17) now designated Nse5 and -6 (formerly Kre29) that are essential in *S. cerevisiae* (18) but not in *S. pombe* (19). Reconstitution experiments with the essential components of the *S. pombe* complex identified two subcomplexes. Smc5, Smc6, and Nse2 form one of these, with Nse2 bound to the coiled-coil region of Smc5, whereas Nse1, -3, and -4 form a second subcomplex (10). In *S. pombe*, Nse5 and -6 form a third subcomplex (19). The sequence of Nse1 suggests that it may be an E3 ubiquitin ligase, whereas Nse2 is a SUMO ligase (18, 20, 21). Nse3 is related to the MAGE protein family (10), but no sequence motifs have been identified in Nse4 (previously designated Rad62) (16), Nse5, or Nse6. Convincing evidence for a mechanism by which the three subcomplexes interact was not clear from previous studies (10, 19).

Although there is no evidence to suggest whether the Smc5-Smc6 complex does or does not form a ringlike structure, it was

* This work was supported by a Medical Research Council Programme Grant and by the European Community Risc-Rad Integrated Project. The costs of publication of this article were defrayed in part by the payment of page charges. This article must therefore be hereby marked "*advertisement*" in accordance with 18 U.S.C. Section 1734 solely to indicate this fact.

[1] Present address: Dept. of Functional Genomics and Proteomics, Masaryk University, Kamenice 5, 625 00 Brno, Czech Republic.

[2] To whom correspondence should be addressed: Genome Damage and Stability Centre, University of Sussex, Falmer, Brighton BN1 9RQ, United Kingdom. Tel.: 44-1273-678120; Fax: 44-1273-678121; E-mail: a.r.lehmann@sussex.ac.uk.

[3] The abbreviations used are: SMC, structural maintenance of chromosomes; E3, ubiquitin-protein isopeptide ligase; aa, amino acid(s); GST, glutathione *S*-transferase.

TABLE 1
Primers used for site-directed mutagenesis

Mutation	Primer (forward/reverse)
L215N	CCT CAA ACA GTG GAG AAC aac TTT TAT GTC AGC TTT TTA TTC GAA TAA AAA GCT GAC ATA AAA gtt GTT CTC CAC TGT TTG AGG
F216A	CAA ACA GTG GAG AAC TTG gcT TAT GTC AGC TTT TTA TTC GAA TAA AAA GCT GAC ATA Agc CAA GTT CTC CAC TGT TTG
F216N	CAA ACA GTG GAG AAC TTG aaT TAT GTC AGC TTT TTA TTC GAA TAA AAA GCT GAC ATA Att CAA GTT CTC CAC TGT TTG
Y217N	CCT CAA ACA GTG GAG AAC TTG TTT aAT GTC AGC TTT TTA TTC AAA GAA GGC GCC TTC TTT GAA TAA AAA GCT GAC ATt AAA CAA GTT CTC CAC TGT TTG AGG
V218N	CA GTG GAG AAC TTG TTT TAT aaC AGC TTT TTA TTC AAA GAA GGC AAA GCT GCC GGC AGC TTT GCC TTC TTT GAA TAA AAA GCT Gtt ATA AAA CAA GTT CTC CAC TG
S219A	CA GTG GAG AAC TTG TTT TAT GTC gcC TTT TTA TTC AAA GAA GGC AAA GCT GCC GGC AGC TTT GCC TTC TTT GAA TAA AAA Ggc GAC ATA AAA CAA GTT CTC CAC TG
S219D	CA GTG GAG AAC TTG TTT TAT GTC gaC TTT TTA TTC AAA GAA GGC AAA GCT GCC GGC AGC TTT GCC TTC TTT GAA TAA AAA Gtc GAC ATA AAA CAA GTT CTC CAC TG
F220N	C TTG TTT TAT GTC AGC aaT TTA TTC AAA GAA GGC AAA G C TTT GCC TTC TTT GAA TAA Att GCT GAC ATA AAA CAA G
L221N	G TTT TAT GTC AGC TTT aac TTC AAA GAA GGC AAA GCT GCC CTCG C GAG GGC AGC TTT GCC TTC TTT GAA gtt AAA GCT GAC ATA AAAC
F222N	G TTT TAT GTC AGC TTT TTA aaC AAA GAA GGC AAA GCT GCC CTC G C GAG GGC AGC TTT GCC TTC TTT Gtt TAA AAA GCT GAC ATA AAA C
K223E	GTC AGC TTT TTA TTC gAA GAA GGC AAA GCT GCC GGC AGC TTT GCC TTC TTc GAA TAA AAA GCT GAC

of interest to determine if any of the Nse proteins fulfilled a kleisin-like function, interacting with the head regions of Smc5 and/or Smc6. This would assign it to a hypothetical kleisin δ subfamily (6). In this paper, we show that *S. pombe* Nse4 is a strong candidate for this role. Nse4 binds to both Smc5 and Smc6, and structural modeling suggests that the C-terminal domain of Nse4 can be folded into a winged helix structure similar to the C terminus of Scc1, which interacts with Smc1. We show that critical residues in this motif destroy the interaction of Nse4 with Smc5, while maintaining its interaction with Nse3. In addition, we find that Nse3, as well as Nse5 and Nse6, although unrelated to kleisin structures, also bind to the head regions of Smc5 and -6.

EXPERIMENTAL PROCEDURES

Plasmid Constructs—The following constructs were used: for Nse3, see Ref. 10; for Nse4, pGBKT7-Nse4-(1–300), pGBKT7-Nse4-(1–150), and pGBKT7-Nse4-(144–300); for Nse5, pGEX-KG-Nse5-(1–388); for Nse6, pGBKT7-Nse6-(1–522); for Smc5, pRSF-Duet-Smc5-(1–1065), pTriEx-4-Smc5-(171–910), pTriEx-4-Smc5-(1–225 plus 837–1065), and pTriEx-4-Smc5-(1–225 plus 837–1010); and for Smc6, pTriEx-4-Smc6-(260–979), pTriEx-4-Smc6-(1–294 plus 896–1140), and pTriEx-4-Smc6-(1–410 plus 875–1140).

Nse4—PCR and standard cloning procedures were used. The Nse4 open reading frame was amplified from a pDB20-cDNA *S. pombe* library and subcloned into pGBKT7 (10). A DNA fragment coding aa 1–150 was PCR-amplified (using JP163 5′-A ACC ATG GCC ATG TCC TCC ATT GAT AAA CGG-3′ and JP190 5′-T CTC GAG TCA CCG CTG GAT GTT TCT TTC TTT) and subcloned into pGEM-T-Easy (Promega). An NcoI-XhoI fragment was then inserted into pGBKT7 two-hybrid vector (Clontech). A DNA fragment coding aa 144–300 was PCR-amplified (using JP163 (5′-A ACC ATG GCC AAA GAA AGA AAC ATC CAG CGG CGA-3′) and JP169 (5′-T CTC GAG GCC ATA CCA AGT ATT ACT GTT AGT-3′)) and subcloned into pGEM-T-Easy. An NcoI-EcoRI fragment was then inserted into pGBKT7 two-hybrid vector. Site-directed mutagenesis (Stratagene) was used to mutate Nse4 residues in the pGBKT7-Nse4-(1–300) construct (Table 1).

Nse5—Nse5 was amplified from cDNA and cloned into pGEX-KG using NcoI and SalI sites. The following primers were used for PCR amplification: 5′-CCT TCT TCC CCC ATG GCT ATG AAC TCG GCT CTA AAG GCA ATA-3′ and 5′-CCT TCT TCC CGT CGA CTT AAA CGA TTT TAT CCA AGG ACA A-3′.

Nse6—Nse6 was amplified from c-DNA and cloned into pGEX-KGH vector using NdeI-XhoI sites. The primers used were as follows: 5′-CTT CTT CCC CAT ATG AAT GCG TCT AAT AAC ATT TCA-3′ and 5′-CTT CTT CCC CTC GAG TTA TCT TTT GTA CGC TTG CCG TTT-3′.

Smc—Smc5 "headless" (aa 171–910) fragment was amplified using primers JP261 (5′-GAC GAC GAC AAG ATG GCA CAT GAG AAG CTT ATT GAT-3′) and JP262 (5′-GAG GAG AAG CCC GGT TCA AGA AAA TCT ATC GCT AAT ACA-3′). The fragment was cloned into pTriEx-4 vector using the ligation-independent cloning protocol (Novagen). To clone pTriEx-4-Smc5 "heads," we amplified sequences encoding the N-terminal (aa 1–225) and C-terminal (aa 837–1065) domains and connected them by a sequence encoding a FLAG tag and tobacco etch virus cleavage site (4). The following pairs of oligonucleotides were used as primers: JP416 (5′-GAC GAC GAC AAG ATG ATC TTA ACA CGC GAG AGT TAC-3′) and JP170 (5′-T GTC GAC TTT ATC GTC ATC ATC TTT ATA CAT TTC GAT GTA TGA TTT GAT TTT T-3′); JP173 (5′-TCC ATG GTC GAC GAA AAC CTG TAT TTT CAG GGC AAC AAA ATT AGC ATC GAA GAA ACG A-3′) and JP417 (5′-GAG GAG AAG CCC GGT TCA TTA TGA CGA AGA AAT GAG TGC GG-3′). To make a truncated version of the Smc5 heads pTriEx-4-Smc5-(1–225 plus 837–1010), we amplified the heads construct using primers JP416 and JP418 (5′-GAG GAG AAG CCC GGT TCA AAC AGC GTT GTC ACA CAC TG-3′). To clone pTriEx-4-Smc5 heads with 150-aa-long coiled-coil fragment, we amplified sequences encoding the N-terminal (aa 1–323) and C-terminal (aa 732–1065) domains

and connected them by a sequence encoding a FLAG tag and tobacco etch virus cleavage site. The following pairs of oligonucleotides were used as primers: JP416 and JP176 (5′-T GTC GAC TTT ATC GTC ATC ATC TTT ATA TCG ATT GGT ATT AAC CTT CTC ATA 3′); JP179 (5′-TCC ATG GTC GAC GAA AAC CTG TAT TTT CAG GGC AAT TCG GTG TTA AAA GTT AAG GAG-3′) and JP417.

Smc6—Smc6 headless (aa 260–979) fragment was amplified using primers JP174 (5′-GAC GAC GAC AAG ATG AAA GGA ATT CAG CTG AAA CAG-3′) and JP175 (5′-GAG GAG AAG CCC GGT TCA CAT TTC ATT ACG CCT TCG TAA-3′). The fragment was cloned into pTriEx-4 using the ligation-independent cloning protocol (Novagen). To clone Smc6 heads, we amplified sequences encoding the N-terminal (aa 1–294) and C-terminal (aa 896–1140) domains and connected them by a sequence encoding a FLAG tag and tobacco etch virus cleavage site (4). The following pairs of oligonucleotides were used as primers: JP443 (5′-GAC GAC GAC AAG ATG ACT ACA GAG CTT ACT AAT G-3′) and JP184 (5′-T GTC GAC TTT ATC GTC ATC ATC TTT ATA AGA GAC CCC AGT TTT CTT ATT TCC T-3′); JP187 (5′-TCC ATG GTC GAC GAA AAC CTG TAT TTT CAG GGC ACA GCA AAG GCT AAT ACT CGC TGT G-3′) and JP442 (5′-GAG GAG AAG CCC GGT TCA TGG CGC CGT AGA GGG AGG AAG-3′). To clone pTriEx-4-Smc5 heads with a longer coiled-coil fragment (aa 1–410 and aa 875–1140), the following pairs of oligonucleotides were used as primers: JP443 and JP448 (5′-CCC TTT ATC GTC ATC ATC TTT ATA ATC ATT CAT TTC TGA ACG ATA CCC-3′); JP449 (5′-GGG TTT GAA AAC CTG TAT TTT CAG GGC ACC AAT ATT TTG CGT GAA AAG G-3′) and JP442.

In Vitro Transcription-Translation—Open reading frames corresponding to proteins or protein fragments were amplified from *S. pombe* cDNAs (10) and expressed *in vitro* as Myc-, hemagglutinin-, S-, or untagged proteins from the pGBKT7, pGADT7, or pTriEx-4 vector by use of the TNT Quick coupled transcription-translation system (Promega) in 50-μl reactions according to the manufacturer's instructions.

Myc Pull-down Experiments—For Myc pull-down experiments, 10–50 μl of in vitro expressed proteins in a total volume of 250 μl of HEPES buffer C (25 mM HEPES (pH 7.5), 200 mM KCl, 3 mM $MgCl_2$, 10% glycerol, 1 mM dithiothreitol, 1 mM phenylmethylsulfonyl fluoride, 0.2% Nonidet P-40, and protease inhibitors) were mixed with 10 μl of an anti-Myc monoclonal antibody and incubated overnight at 4 °C. Fifty μl of protein G-Sepharose beads (CRUK, London) were then added, and the mixture was incubated for 2 h. The beads were washed three times with HEPES buffer C containing 300 mM NaCl. Input, unbound, and bound fractions were separated by SDS-PAGE and analyzed by phosphorimaging.

GST Pull-down Experiments—The pGEX-Nse5 construct was expressed in BL21 cells. Cells were induced with 0.2 mM isopropyl 1-thio-β-D-galactopyranoside and harvested after 3–4 h of induction. Bacteria were lysed in HEPES Buffer C with protease inhibitors. GST-Nse5 fusion protein was then immobilized on glutathione-Sepharose beads (50 μl; Novagen) and incubated with 10–50 μl of *in vitro* expressed proteins in a total volume 250 μl of HEPES Buffer C overnight at 4 °C. Bound proteins were analyzed as described above.

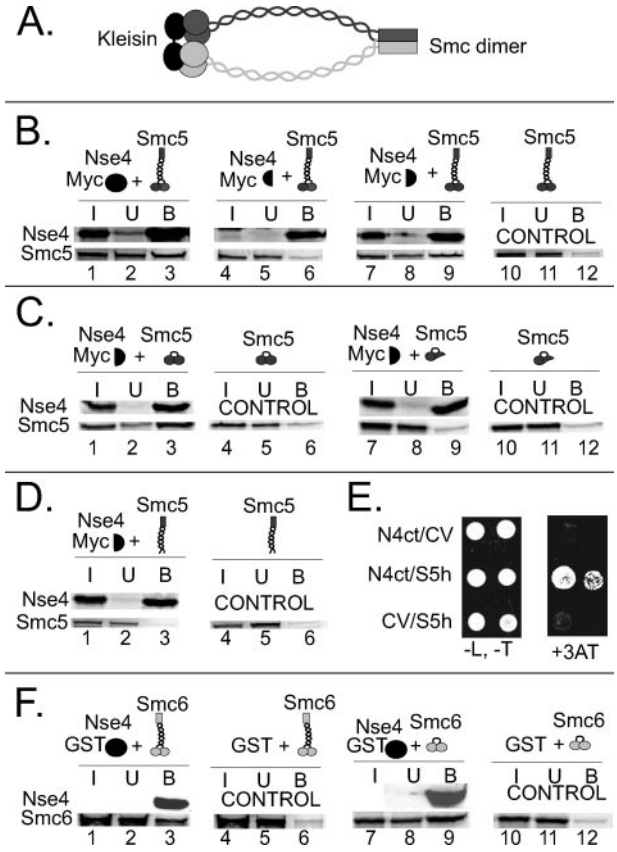

FIGURE 1. **Nse4 binds to the head domains of Smc5.** *A*, schematic of the structures of Smc heterodimers and kleisin. *B*, Smc5 was mixed with full-length (*lanes 1–3*), N-terminal (aa 1–150; *lanes 4–6*), or C-terminal fragment (aa 144–300; *lanes 7–9*) of Myc-Nse4 and incubated with anti-Myc antibody overnight. In the control experiment, the Smc5 protein was incubated with antibody and beads in the absence of Myc-Nse4 (*lanes 10–12*). Input (*I*), unbound (*U*), and bound (*B*) fractions were collected and run in SDS-10% polyacrylamide gels. Unbound and input fractions can be compared directly and represent one-twentieth of the total reaction mix, whereas the bound fraction represents about one-third of the reaction. *C*, the C-terminal Myc-Nse4 fragment was mixed with either the Smc5 heads construct (aa 1–225 plus aa 837–1065; *lanes 1–6*) or the same construct missing aa 1011–1065. *D*, the C-terminal Myc-Nse4 fragment was mixed with the Smc5 headless fragment containing aa 170–910 (*lanes 1–6*). *E*, yeast two-hybrid analysis of interactions between Nse4 C-terminal fragment (*N4ct*) and Smc5 heads (*S5h*). In each set, the *left panel* shows a positive control of cells growing in medium lacking leucine (−*L*) or tryptophan (−*T*), and the *right panel* shows growth in selective medium containing 3-aminotriazole (+*3AT*). Results for two concentrations of cells differing by a factor of 10 are shown. In each case, controls (*CV*) with appropriate empty vectors are provided *above* and *below* the test pairs. *F*, GST-tagged Nse4 (*lanes 1–3* and *7–9*) or GST alone (*lanes 4–6* and *10–12*) were mixed with full-length (*lanes 1–6*) or heads construct (*lanes 7–12*) of Smc6.

Yeast Two-hybrid Analysis—The Matchmaker Gal4 two-hybrid system 3 (Clontech) was used to analyze interactions between the individual components of the *S. pombe* complex. Transformation of the constructs cloned in pGBKT7, pGADT7, and/or pACT2 into *S. cerevisiae* Y190 and growth on selective media were performed according to the manufacturer's instructions.

Site-directed Mutagenesis—The QuikChange II XL system (Stratagene) was used to create point mutations within the Nse4 open reading frame, using primers listed in Table 1.

Bioinformatics—The PSIPRED algorithm (available on the World Wide Web at bioinf.cs.ucl.ac.uk/psipred) was used to

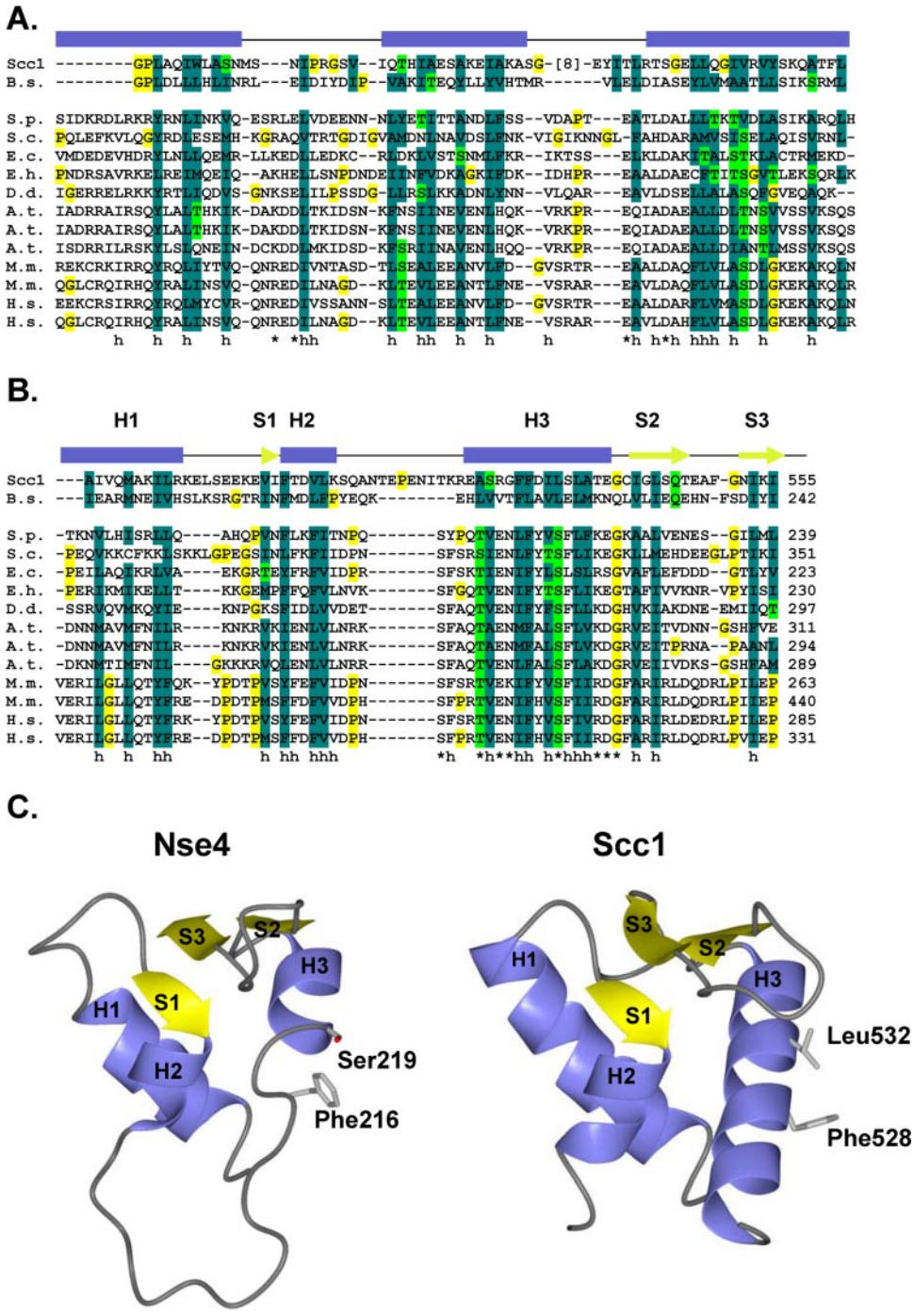

FIGURE 2. **Nse4 proteins are δ-kleisin subunits of Smc5-Smc6 complexes.** *A* and *B*, alignment of N-terminal (*A*) and C-terminal (*B*) domains of Nse4 orthologs, indicating putative helix-turn-helix motifs (*A*) and winged helix domain (*B*). Also shown in the *top two lines* are *B. subtilis* kleisin ScpA (*B.s.*) and *S. cerevisiae* Scc1. Nse4 orthologs are from *S. pombe* (*S.p.*), *S. cerevisiae* (*S.c.*), *Encephalitozoon cuniculi* (*E.c.*), *Entamoeba histolytica* (*E.h.*), *Dictyostelium discoideum* (*D.d.*), *Arabidopsis thaliana* (*A.t.*), *Mus musculus* (*M.m.*), *Homo sapiens* (*H.s.*). *Shading* represents amino acid groups conserved across the kleisin superfamily, as shown in Schleiffer *et al.* (6). *Dark green*, hydrophobic; *light green*, hydrophilic. All glycine and proline residues are *highlighted in yellow*, and most are located in the putative loops. *h*, hydrophobic; *, other residues conserved in Nse4 orthologs. *C*, comparison of the structure of Scc1 with the predicted structure of the C terminus of Nse4.

analyze the protein secondary structure (22). The homology model of Nse4 (Fig. 2*C*) was constructed using the SWISS-MODEL automated protein structure homology-modeling server (available on the World Wide Web at swissmodel.expasy.org) (23) using the crystal structure of *S. cerevisiae* Scc1 (Protein Data Bank code 1w1w) as the template structure.

Monitoring of Septation and Mitotic Indices—Approximately 5×10^8 cells were collected by centrifugation (4 min, 5000 rpm), resuspended in 100 μl of methanol, and incubated at 4 °C overnight. 10 μl of these fixed cells were transferred onto microscope slides and stained with 100 μl/ml 4′,6-diamidino-2-phenylindole and 50 μg/ml Calcofluor in mounting medium (1 mg/ml *n*-propyl-gallate, 1 mg/ml *p*-phenyl-enediamine in glycerol/PBS (9:1)). The proportion of cells with a septum or "mitotic phenotype" was determined on a fluorescence microscope, scoring a minimum of 300 cells/sample.

Analysis of Nse4 Protein Levels during Cell Cycle and after Exposure to DNA Damage—For cell cycle experiments, *S. pombe cdc25.22* cells in midlog phase were synchronized at the G_2/M boundary by shifting them from 25 to 36 °C for 4 h. Following return to permissive temperature, the passage of the cells through the cell cycle was followed for 5 h, taking samples every 20 min. At each time point, the septation index was also determined. For exposure to hydroxyurea, cells from *S. pombe* strain MMP21 containing an integrated copy of C-terminally FLAG-tagged Nse4 (16) were incubated, in midexponential growth, in the presence of 10 mM hydroxyurea for 4 h. The cells were released from the hydroxyurea block by washing them once in culture medium, and progression through one cell cycle was followed for 3 h. Samples were taken every 15 min. For γ-irradiation, MMP21 cells grown to A_{600} = 1.0 were irradiated with 500 grays of γ-irradiation. Protein levels were analyzed in nonirradiated control cells and cells recovering from irradiation for different times. For estimation of Nse4 protein levels in the above experiments, 50 A_{600} of cells were collected, and after a rinse in 1 ml of H_2O, the cells were disrupted with glass beads in 200 μl of 20% trichloroacetic acid in a Ribolyser (3 × 15 s, 6500 rpm). After centrifugation, the precipitated protein was washed from the glass beads with 400 μl of 5% trichloroacetic acid, pelleted by centrifugation (5 min, 13,000 rpm), and resuspended in Laemmli buffer, and where necessary the pH was adjusted to 6.8.

Proteins were resolved by SDS-PAGE, and the protein levels of Nse4 were monitored by immunoblotting and probing with Nse4-specific antiserum generously supplied by T. Morishita and H. Shinagawa. Additionally, the levels of Cdc2 kinase were monitored in parallel with Cdc2 p34 antiserum (Santa Cruz Biotechnology, Inc., Santa Cruz, CA) as a loading control.

RESULTS

Interaction of Nse4 with Smc5 and Smc6—In an attempt to find the missing link between the Smc6-Smc5-Nse2 and Nse1-Nse3-Nse4 subcomplexes (10), *in vitro* transcription-translated proteins were used in pull-down assays. When extracts of Myc-Nse4 and Smc5 (full-length) were incubated together overnight with anti-Myc antibody, most of the Nse4 was in the bound fraction after precipitating the immune complex with protein G-Sepharose beads (Fig. 1*B*, *lane 3*, *top panel*). A significant proportion of Smc5 was also pulled down in an Nse4-dependent manner (Fig. 1*B*, compare *lanes 3* and *12*, *bottom panel*). To see which part of Nse4 was involved in binding to Smc5, we generated two Myc-tagged fragments of Nse4, from aa 1 to 150 (nt) and from aa 144 to 300 (ct). Smc5 bound only to the C-terminal fragment (Fig. 1*B*, *lane 9*, *bottom panel*), not to the N-terminal fragment (*lane 6*, *bottom panel*) or to beads alone (*lane 12*).

To investigate which part of Smc5 is involved in the interaction with Nse4, we generated heads and headless constructs of Smc5. Smc5 heads contained the globular N- and C-terminal domains joined by a short coiled-coil region and a linker. The Smc5 headless construct lacked the globular heads and contained the central coiled-coil together with the hinge domain. In immunoprecipitation assays using the Nse4-ct and Smc5 heads, Smc5 heads bound to the beads (Fig. 1*C*, *lane 3*, *bottom panel*; compare control in *lane 6*). In contrast, the Smc5 headless protein did not bind to the beads (Fig. 1*D*, *lane 3*, *bottom panel*). In order to confirm our pull-down data, we used the yeast two-hybrid system. Nse4 and Smc5 genes were fused to the Gal4 binding and activation domains, respectively, and cotransformed into the Y190 budding yeast strain. Nse4-Smc5 interaction-dependent transcriptional activation of the *HIS3* gene was seen with full-length proteins as well as with Nse4-ct and Smc5 heads (Fig. 1*E*; see also Fig. 3). We conclude that there is an interaction between Nse4 and Smc5 that is mediated by the C-terminal half of Nse4 and the heads domain of Smc5.

In similar experiments to those described above, we examined the interaction of GST-Nse4 with Smc6. We were able to show that GST-tagged Nse4 interacted with full-length Smc6 (Fig. 1*F*, *lane 3*, *lower panel*) and with Smc6 heads (*lane 9*) but not with headless Smc6 (data not shown). GST alone did not bind to any of the constructs (Fig. 1*F*, *lanes 6* and *12*).

Nse4 Structure Is Similar to That of Other Kleisins—Our finding that Nse4 binds to the globular heads of both Smc components of the Smc5-Smc6 complex is reminiscent of the behavior expected of kleisins. In cohesin, an N-terminal helix-turn-helix domain of the kleisin Scc1 interacts with Smc3 heads, whereas a C-terminal winged helix domain (24), composed of three helices followed by two β-sheets, interacts with the two most C-terminal β-sheets of Smc1 (25). Our results suggested that Nse4 protein might bind to the Smc5-Smc6 heterodimer in a similar manner. Indeed, the PSIPRED secondary structure prediction program (22) identified a putative helix-turn-helix motif in the N-terminal halves of Nse4 orthologs (Fig. 2*A*) and a winged helix motif in the C-terminal halves (Fig. 2*B*). The conserved hydrophobic patterns of the Nse4 structural elements (*dark green* in Fig. 2, *A* and *B*) are also similar to hydrophobic patterns characteristic for the whole kleisin family (6). To determine if Nse4 showed significant similarity to non-Nse4 proteins in the protein sequence data base, we performed iterative PSI-BLAST data base searches using the sequences of the *S. pombe* and *S. cerevisiae* Nse4 proteins. These searches revealed that Nse4 displayed no significant sequence similarity to other non-Nse4 proteins. Next, we employed sequence-threading algorithms to predict if Nse4 displayed a similar structural organization to other proteins in the protein structural data base (Protein Data Bank). When the yeast Nse4 sequences were compared with the secondary structure and fold data bases using the protein fold recognition algorithms PSIPRED and PHYRE (22, 26), the C-terminal halves were predicted to adopt structures most similar to the winged helix domain of Scc1 (Fig. 2*C*) as well as to a number of other winged helix domain proteins.

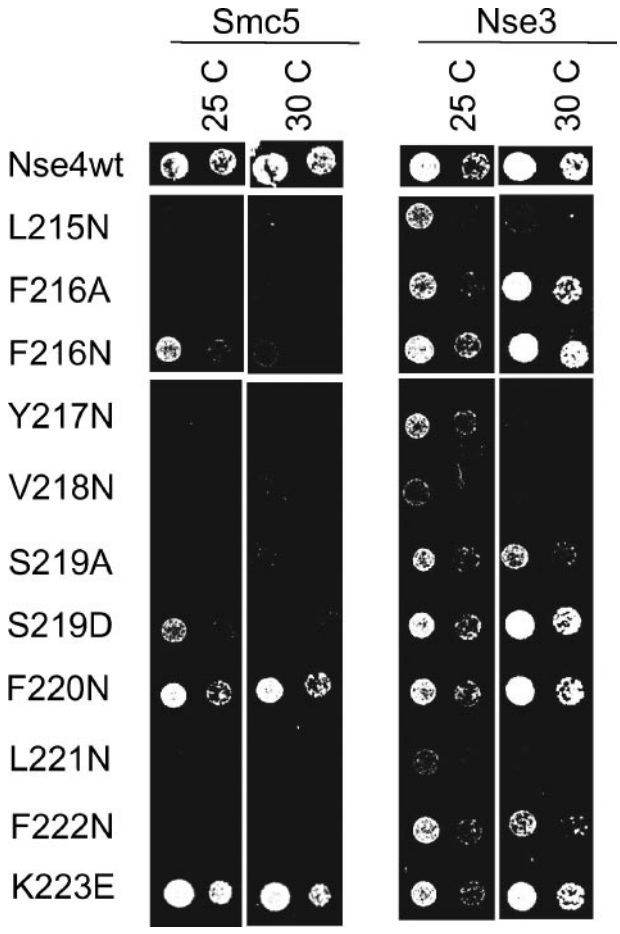

FIGURE 3. **Mutations in H3 recognition helix of winged helix domain disrupt the Nse4 interaction with Smc5.** Analysis of mutants of Nse4 mutated in the putative H3 motif using the yeast two-hybrid system is shown. The *two left-hand panels* show interactions with Smc5 at 25 and 30 °C; the *two right-hand panels* show interactions with Nse3. In each case, two dilutions of the cells were used.

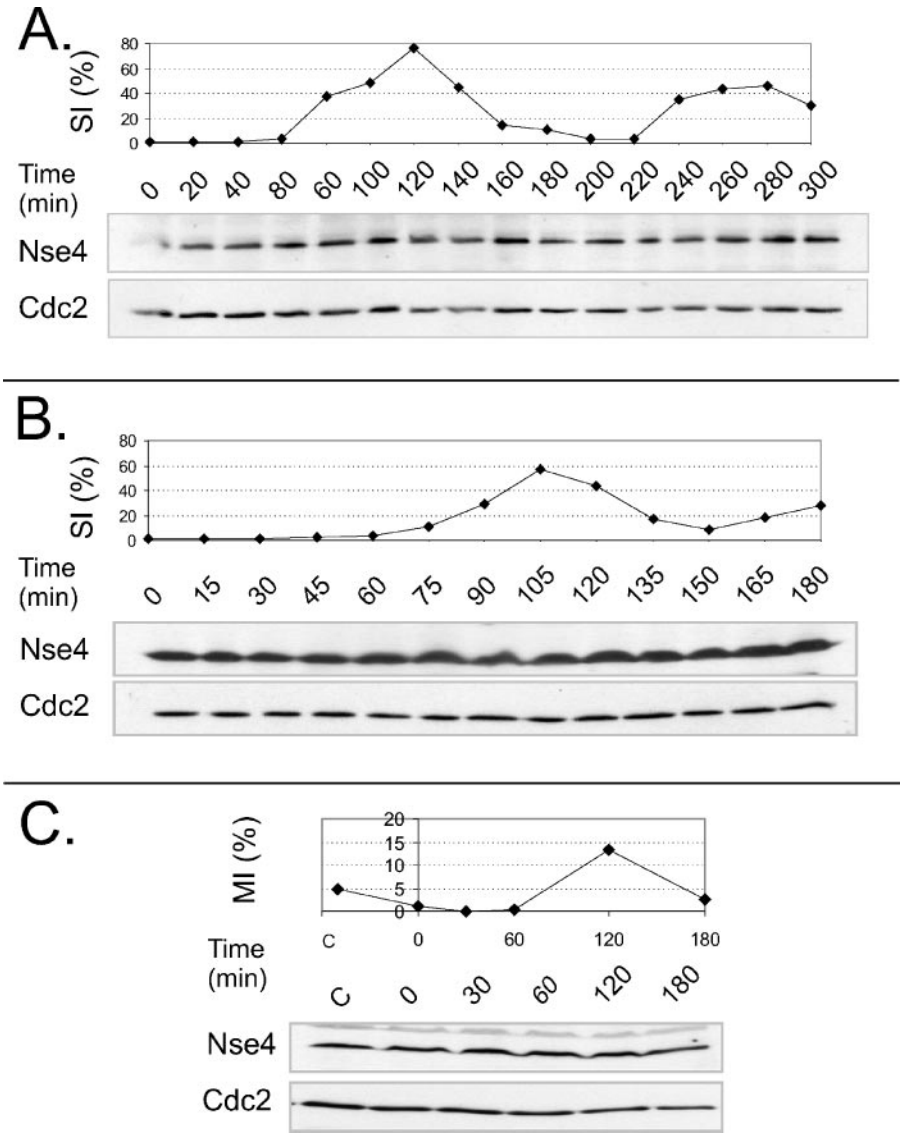

FIGURE 4. **Nse4 protein content remains constant during progression through cell cycle and after γ-irradiation.** *A*, *S. pombe cdc25.22* cells synchronized at the G_2/M boundary by shifting them from 25 to 36 °C were returned to permissive temperature, and the levels through the cell cycle of Nse4 and Cdc2 (used as a loading control) were visualized by immunoblotting with anti-Nse4 antibody. At each time point, the septation index (*SI*) was also determined. *B*, cells from *S. pombe* strain MMP21 containing an integrated copy of C-terminally FLAG-tagged Nse4 (16) were incubated in 10 mM hydroxyurea for 4 h. After release from the hydroxyurea block, samples were analyzed as described for *A*. *C*, MMP21 cells grown to $A_{600} = 1.0$ were irradiated with 500 grays of γ-irradiation. Nse4 and Cdc2 protein levels were analyzed in nonirradiated control cells (*C*) and in cells recovering from irradiation. In addition, the mitotic index (*MI*) was monitored.

The Scc1 crystal structure revealed that Phe[528] and Leu[532] residues of the third helix (H3; aa 522–535 in *S. cerevisiae*) make physical contacts with Smc1 head residues (25) (Fig. 2*C*, *right*). To test whether similar residues in the predicted Nse4 winged helix motif interact with Smc5, we performed site-directed mutagenesis of most of the residues in the putative Nse4 helix H3 (aa 208–223 in *S. pombe*). We used these mutated Nse4 constructs in a yeast two-hybrid assay to analyze the effect of the mutations on the interaction with Smc5 at both 25 and 30 °C. As a control, we also analyzed their interactions with Nse3 (Fig. 3). Most of the mutant proteins failed to interact with either Nse3 or Smc5 (Fig. 3) (data not shown). We assume that in these cases the mutation caused a general disruption of the structure of the protein. However, mutations at Phe[216], Ser[219], and Phe[222] maintained the interaction with Nse3 but specifically destroyed the interaction with Smc5. Mutations at Phe[220] and Lys[223] had no effect on either interaction. These data suggest that Phe[216], Ser[219], and Phe[222] might be critical residues for the interaction with Smc5. Our structural prediction (Fig. 2*C*) shows that Phe[216] and Ser[219] protrude from the face of the protein expected to interact with Smc5.

The interaction between the C-terminal domain of Scc1 and the head domain of Smc1 is mediated by two β-sheets at the extreme C terminus of Smc1. To determine if a similar situation pertained with Smc5, we deleted the C-terminal 55 aa of the Smc5 heads construct and used this in a pull-down assay with Nse4-Ct (Fig. 1*C*, *lanes 7–12*). The Nse4-Ct interacted with Smc5 heads (*lane 3*, *lower panel*) as described above, but deletion of the C-terminal 55 aa of Smc5 abolished this interaction (*lane 9*, *lower panel*). This finding is consistent with the idea that the extreme C terminus of Smc5 interacts with the C terminus of Nse4 as is also the case with Smc1 and Scc1.

Stability of Nse4—Scc1 is cleaved prior to anaphase by separase, a specific protease. We have analyzed the stability of Nse4 through the cell cycle. *cdc25.22* cells were held at the restrictive temperature of 36 °C for 4 h to synchronize cells in late G_2. On release to the permissive temperature, samples were taken every 20 min. We did not detect any change in Nse4 levels through the cell cycle (Fig. 4*A*). We carried out similar experiments after exposing cells to a 4-h treatment with hydroxyurea or to 500 grays of γ-irradiation. In neither case did we detect significant changes in the levels of Nse4 (Fig. 4, *B* and *C*). We conclude that Nse4 is not degraded like Scc1, although our experiments do not exclude the possibility of minor fluctuations in the cellular content of Nse4.

Interactions of Nse3—Since Nse4 is in a subcomplex with Nse3 and Nse1 (10), we also investigated the binding of Nse3 to Smc5 and -6. We found that GST-tagged Nse3, like Nse4, bound to both Smc5 (Fig. 5*A*, *lane 3*) and Smc6 (Fig. 5*C*, *lane 3*). Nse3 bound to the heads (Fig. 5*B*, *lane 3*) but not the headless construct of Smc5 (Fig. 5*A*, *lane 9*). Interestingly, and in contrast to the binding of Nse4, deletion of the C-terminal 55 aa of

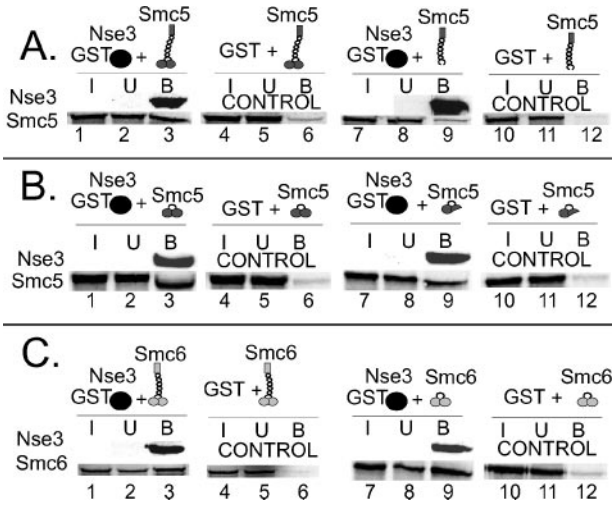

FIGURE 5. **Interaction of Nse3 with Smc5 and 6.** *A*, GST-Nse3 interacts with full-length Smc5 (*lanes 1–6*) but not with headless Smc5 (*lanes 7–12*). *B*, Nse3 interacts with the heads construct of Smc5 (*lanes 1–6*) and with the same construct lacking the C-terminal 55 aa (*lanes 7–12*). *C*, Nse3 interacts with full-length Smc6 (*lanes 1–6*) and Smc6 heads (*lanes 7–12*).

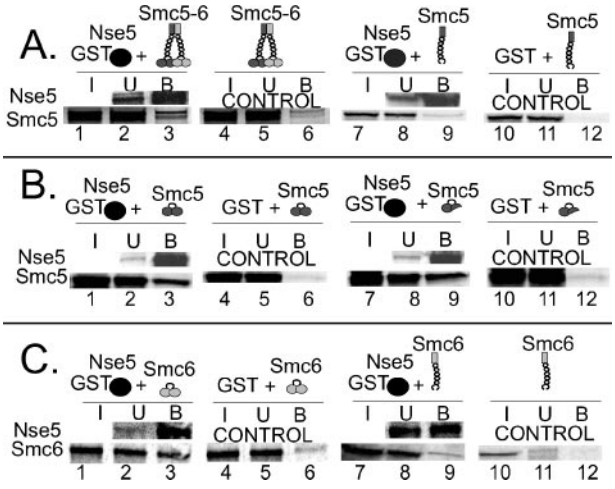

FIGURE 6. **Interaction of Nse5 with Smc5 and -6.** *A*, GST-Nse5 interacts with full-length Smc5-Smc6 (*lanes 1–6*) but not with headless Smc5 (*lanes 7–12*). *B*, Nse5 interacts with the heads construct of Smc5 (*lanes 1–6*) and with the same construct lacking the C-terminal 55 aa (*lanes 7–12*). *C*, Nse5 interacts with Smc6 heads (*lanes 1–6*) but not with headless Smc6 (*lanes 7–12*).

Smc5 did not affect its binding to Nse3 (Fig. 5*B*, *lane 9*). Binding was also seen with Smc6 heads (Fig. 5*C*, *lane 9*) but not with the headless construct (not shown). Thus, although Nse3, like Nse4, also bridged the heads of Smc5 and -6, the binding site on Smc5 appears to be different from that of Nse4. Furthermore, structural predictions did not reveal any kleisin-like features in Nse3.

Interaction of Nse5 and Nse6 with Smc5 and Smc6—Recently, Pebernard *et al.* (19) identified the two nonessential components, Nse5 and Nse6, from the *S. pombe* Smc5-Smc6 complex. They showed that Nse5 and Nse6 interacted with full-length Smc5 and Smc6 and proposed that it was these proteins that performed the kleisin-like function of bridging the head domains of Smc5 and -6. In confirmation of their findings, we observed that GST-tagged Nse5 was indeed able to pull down full-length Smc5 and Smc6 (Fig. 6*A*, *lane 3*). However, it did not bind to the headless Smc5 protein (*lane 9*). Nse5, like Nse4,

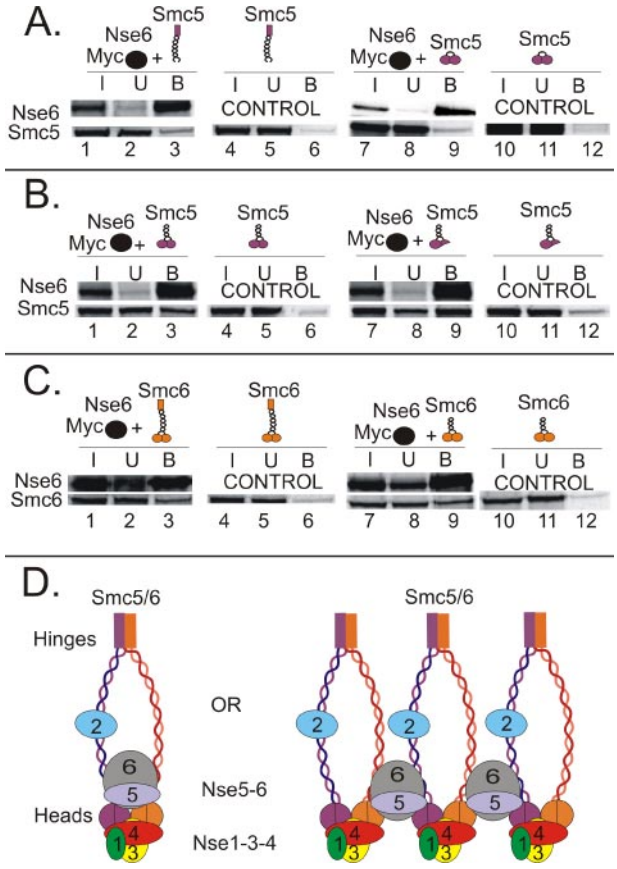

FIGURE 7. **Interaction of Nse6 with Smc5 and -6.** *A*, no interactions of Myc-Nse6 with Smc5 headless (*lanes 1–6*) or heads (*lanes 7–12*). *B*, interaction of Nse6 with the heads construct of Smc5 with approximately 150 aa of coiled-coil arms (*lanes 1–6*) and with the same construct lacking the C-terminal 55 aa (*lanes 7–12*). *C*, Nse6 interacts with full-length Smc6 (*lanes 1–6*) and with the heads construct attached to approximately 100 aa of coiled-coil (*lanes 7–12*). *D*, models for architecture of the Smc5-Smc6 complex.

bound to Smc5 heads (Fig. 6*B*, *lane 3*), but, as with Nse3 and unlike with Nse4, this binding was unaffected by deletion of the C-terminal 55 aa of Smc5 (*lane 9*). GST-tagged Nse5 also bound to Smc6 heads (Fig. 6*C*, *lane 3*) but not to headless Smc6 (*lane 9*). These findings show that Nse5 also binds to Smc5 and Smc6, but this binding occurs at a site on Smc5 distinct from the binding site of Nse4.

Nse6 also bound to both Smc5 and Smc6, but the binding sites differed slightly from that of the other Nse proteins. Nse6 bound to full-length Smc5 (not shown), but there was no significant binding to either headless (Fig. 7*A*, *lane 3*) or heads constructs (*lane 9*). In the heads constructs used in all experiments described so far, the globular N- and C-terminal heads were attached to ~50 aa of each coiled-coil arm, joined by a linker. We made a new construct in which the coiled-coil arms attached to the heads were increased to approximately 150 aa. Nse6 did bind to this construct (Fig. 7*B*, *lane 3*). As with binding to Nse3 and Nse5, the C-terminal 55 aa of Smc5 were dispensable for binding to Nse6 (Fig. 7*B*, *lane 9*). In a similar manner, Nse6 bound to full-length Smc6 (Fig. 7*C*, *lane 3*) and a construct in which the heads were attached to approximately 100 aa of coiled-coil domains (Fig. 7*C*, *lane 9*), but there was no interaction with the Smc6 heads or headless constructs (data not shown).

DISCUSSION

In the cohesin complex, the non-SMC proteins Scc1 and Scc3 bind to the heads of Smc1 and -3, but only Scc1 makes direct contact with Smc1 and -3. Scc1 is the founding member of the kleisin superfamily. In this paper, we have provided evidence that at least four of the six non-Smc (Nse) components of the Smc5-Smc6 complex directly contact both Smc5 and Smc6. Nse4 not only binds to the heads of Smc5 and Smc6, but structural predictions suggest that it is related to Scc1, with a helix-turn helix motif at the N terminus and winged helix domain at the C terminus, which binds to Smc5. We therefore propose that Nse4 is the kleisin subunit of the Smc5-Smc6 complex.

We have confirmed the finding of Pebernard *et al.* (19) that the nonessential Nse5 and Nse6 also bound to both Smc5 and Smc6 (Figs. 6 and 7), but we find that these proteins bound at a distinct site from Nse4. Binding of Nse6 to Smc5 and -6 extends further than the other proteins, away from the heads along the coiled-coils.

Cohesin is thought to form a ring structure whose closure is mediated by Scc1 (4). At the metaphase-anaphase transition, cohesin is cleaved by separase (5), allowing the opening of the ring so that sister chromatids can separate. The ability of Nse4 to bind both Smc5 and Smc6 raised the possibility that the complex might, like cohesin, form a ring whose closure is mediated by Nse4. However, we have not detected any cleavage of Nse4 under a variety of conditions, and even if Nse4 were cleaved, Nse3, -5, and -6 would presumably still bridge the Smc5-Smc6 heads. Opening of the ring would have to occur either by some complex regulation allowing all of these proteins to be removed so that opening of the heads domain can occur or maybe more likely by opening at the hinge domains. If Smc5 and Smc6 do indeed form a ring, we propose, based on our results together with those of Pebernard *et al.* (19), a model for the architecture of the complex shown in Fig. 7*D* (*left*) with the Nse1-Nse3-Nse4 subcomplex binding on the "outside" surface of the heads and the Nse5-Nse6 subcomplex binding to the "inside." This binding site of Nse5-Nse6 is reminiscent of the binding of Mre11 to Rad50 in the Rad50-Mre11-Xrs2/Nbs1 complex. Rad50 forms a homodimeric structure similar to the SMC heterodimers, and Mre11 binds as a homodimer to the "inside" of the heads and to the attached coiled-coils (27).

There is no independent evidence that Smc5 and -6 do in fact form a ring, and in principle the bridging Nse proteins could join the Smc5 head of one Smc5-Smc6 heterodimer to the Smc6 head of a neighboring heterodimer. Alternatively, some of the proteins (*e.g.* Nse1, -3, and -4) might form an intramolecular bridge, whereas others (*e.g.* Nse5 and -6) could form intermolecular bridges, as exemplified in the *right-hand diagram* in Fig. 7*D*. Another possibility is that the primary function of Nse4 and Nse3 may be to bind the Nse1 putative ubiquitin ligase to the rest of the complex. Our current and future work is aimed at understanding further the relative locations and functions of the various Nse proteins in the Smc5-Smc6 complex.

Acknowledgments—We are grateful to T. Morishita and H. Shinagawa for anti-Nse4 antibody and for MMP21 cells, to Nigel Brissett for assistance in preparing Fig. 2C, and to Lara Boyd and Felicity Watts for constructs.

REFERENCES

1. Losada, A., and Hirano, T. (2005) *Genes Dev.* **19,** 1269–1287
2. Hirano, T. (2006) *Nat. Rev. Mol. Cell Biol.* **7,** 311–322
3. Nasmyth, K., and Haering, C. H. (2005) *Annu. Rev. Biochem.* **74,** 595–648
4. Gruber, S., Haering, C. H., and Nasmyth, K. (2003) *Cell* **112,** 765–777
5. Uhlmann, F., Wernic, D., Poupart, M. A., Koonin, E. V., and Nasmyth, K. (2000) *Cell* **103,** 375–386
6. Schleiffer, A., Kaitna, S., Maurer-Stroh, S., Glotzer, M., Nasmyth, K., and Eisenhaber, F. (2003) *Mol. Cell* **11,** 571–575
7. Anderson, D. E., Losada, A., Erickson, H. P., and Hirano, T. (2002) *J. Cell Biol.* **156,** 419–424
8. Lehmann, A. R. (2005) *DNA Repair* (*Amst.*) **4,** 309–314
9. Fousteri, M. I., and Lehmann, A. R. (2000) *EMBO J.* **19,** 1691–1702
10. Sergeant, J., Taylor, E., Palecek, J., Fousteri, M., Andrews, E., Sweeney, S., Shinagawa, H., Watts, F. Z., and Lehmann, A. R. (2005) *Mol. Cell Biol.* **25,** 172–184
11. Fujioka, Y., Kimata, Y., Nomaguchi, K., Watanabe, K., and Kohno, K. (2002) *J. Biol. Chem.* **277,** 21585–21591
12. Harvey, S. H., Sheedy, D. M., Cuddihy, A. R., and O'Connell, M. J. (2004) *Mol. Cell Biol.* **24,** 662–674
13. McDonald, W. H., Pavlova, Y., Yates, J. R., III, and Boddy, M. N. (2003) *J. Biol. Chem.* **278,** 45460–45467
14. Hu, B., Liao, C., Millson, S. H., Mollapour, M., Prodromou, C., Pearl, L. H., Piper, P. W., and Panaretou, B. (2005) *Mol. Microbiol.* **55,** 1735–1750
15. Pebernard, S., McDonald, W. H., Pavlova, Y., Yates, J. R., III, and Boddy, M. N. (2004) *Mol. Biol. Cell* **15,** 4866–4876
16. Morikawa, H., Morishita, T., Kawane, S., Iwasaki, H., Carr, A. M., and Shinagawa, H. (2004) *Mol. Cell Biol.* **24,** 9401–9413
17. Hazbun, T. R., Malmstrom, L., Anderson, S., Graczyk, B. J., Fox, B., Riffle, M., Sundin, B. A., Aranda, J. D., McDonald, W. H., Chiu, C. H., Snydsman, B. E., Bradley, P., Muller, E. G., Fields, S., Baker, D., Yates, J. R., III, and Davis, T. N. (2003) *Mol. Cell* **12,** 1353–1365
18. Zhao, X., and Blobel, G. (2005) *Proc. Natl. Acad. Sci. U. S. A.* **102,** 4777–47782
19. Pebernard, S., Wohlschlegel, J., McDonald, W. H., Yates, J. R., III, and Boddy, M. N. (2006) *Mol. Cell Biol.* **26,** 1617–1630
20. Andrews, E. A., Palecek, J., Sergeant, J., Taylor, E., Lehmann, A. R., and Watts, F. Z. (2005) *Mol. Cell Biol.* **25,** 185–196
21. Potts, P. R., and Yu, H. (2005) *Mol. Cell Biol.* **25,** 7021–7032
22. McGuffin, L. J., and Jones, D. T. (2003) *Bioinformatics* **19,** 874–881
23. Schwede, T., Kopp, J., Guex, N., and Peitsch, M. C. (2003) *Nucleic Acids Res.* **31,** 3381–3385
24. Gajiwala, K. S., and Burley, S. K. (2000) *Curr. Opin. Struct. Biol.* **10,** 110–116
25. Haering, C. H., Schoffnegger, D., Nishino, T., Helmhart, W., Nasmyth, K., and Lowe, J. (2004) *Mol. Cell* **15,** 951–964
26. Kelley, L. A., MacCallum, R. M., and Sternberg, M. J. (2000) *J. Mol. Biol.* **299,** 499–520
27. Hopfner, K. P., Karcher, A., Craig, L., Woo, T. T., Carney, J. P., and Tainer, J. A. (2001) *Cell* **105,** 473–485